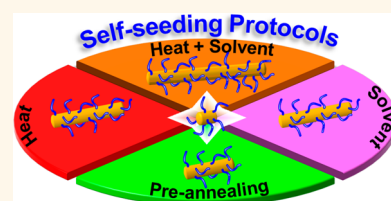


# Self-Seeding in One Dimension: A Route to Uniform Fiber-like Nanostructures from Block Copolymers with a Crystallizable Core-Forming Block

Jieshu Qian,<sup>†,§</sup> Yijie Lu,<sup>†,§</sup> Anselina Chia,<sup>†</sup> Meng Zhang,<sup>†</sup> Paul A. Rupar,<sup>‡,§</sup> Nikhil Gunari,<sup>†</sup> Gilbert C. Walker,<sup>†</sup> Graeme Cambridge,<sup>†</sup> Feng He,<sup>†,||</sup> Gerald Guerin,<sup>†,\*</sup> Ian Manners,<sup>‡,\*</sup> and Mitchell A. Winnik<sup>†,\*</sup>

<sup>†</sup>Department of Chemistry, University of Toronto, 80 St. George Street, Toronto, Ontario, Canada M5S 3H6 and <sup>‡</sup>School of Chemistry, University of Bristol, Bristol BS8 1TS, United Kingdom. <sup>§</sup>These authors contributed equally to this work. <sup>||</sup>Present address: Department of Chemistry, University of Alabama, Tuscaloosa, Alabama 35487. <sup>||</sup>Present address: South University of Science and Technology of China, 1088 Xueyuan Boulevard, Xili, Nanshan, Shenzhen 518055, China.

**ABSTRACT** One-dimensional micelles formed by the self-assembly of crystalline-coil poly(ferrocenylidimethylsilane) (PFS) block copolymers exhibit self-seeding behavior when solutions of short micelle fragments are heated above a certain temperature and then cooled back to room temperature. In this process, a fraction of the fragments (the least crystalline fragments) dissolves at elevated temperature, but the dissolved polymer crystallizes onto the ends of the remaining seed fragments upon cooling. This process yields longer nanostructures (up to 1  $\mu$ m) with uniform width (ca. 15 nm) and a narrow length distribution. In this paper, we describe a systematic investigation of factors that affect the self-seeding behavior of PFS block copolymer micelle fragments. For PI<sub>1000</sub>-PFS<sub>50</sub> (the subscripts refer to the number average degree of polymerization) in decane, these factors include the presence of a good solvent (THF) for PFS and the effect of annealing the fragments prior to the self-seeding experiments. THF promoted the dissolution of the micelle fragments, while preannealing improved their stability. We also extended our experiments to other PFS block copolymers with different corona-forming blocks. These included PI<sub>637</sub>-PFS<sub>53</sub> in decane, PFS<sub>60</sub>-PDMS<sub>660</sub> in decane (PDMS = polydimethylsiloxane), and PFS<sub>30</sub>-P2VP<sub>300</sub> in 2-propanol (P2VP = poly(2-vinylpyridine)). The most remarkable result of these experiments is our finding that the corona-forming chain plays an important role in affecting how the PFS chains crystallize in the core of the micelles and, subsequently, the range of temperatures over which the micelle fragments dissolve. Our results also show that self-seeding is a versatile approach to generate uniform PFS fiber-like nanostructures, and in principle, the method should be extendable to a wide variety of crystalline-coil block copolymers.



**KEYWORDS:** crystalline-coil · block copolymers · self-seeding

Over the past several years, there has been a growing interest in micelle formation by block copolymers in which the crystallinity of the core plays a key role in the self-assembly process.<sup>1</sup> We have referred to this process as crystallization-driven self-assembly (CDSA). Much of this interest has focused on the formation of cylindrical or fiber-like micelles for polymer compositions (*i.e.*, long corona-forming blocks) for which spherical star-like micelles would be predicted if the micelle core were amorphous. Polyferrocenylidimethylsilane<sup>2–4</sup> (PFS) block copolymers are the classic example.<sup>5–8</sup> More recent examples include block copolymers with polyethylene,<sup>9–12</sup> poly(ethylene oxide),<sup>13</sup> poly( $\epsilon$ -caprolactone),<sup>14,15</sup> poly( $\epsilon$ -caprolactone- $b$ -L-lactide),<sup>16</sup> polylactide,<sup>17,18</sup> polyacrylonitrile,<sup>19</sup>

poly(ferrocenylidethyldisilane),<sup>20</sup> poly(ferrocenylidimethylgermane),<sup>21</sup> poly(3-hexylthiophene),<sup>22,23</sup> and poly(perfluorooctylethyl methacrylate)<sup>24</sup> as the core-forming block.<sup>25</sup>

Several of these block polymers have been shown to exhibit seeded growth: If one adds a solution of polymer in a common good solvent to preformed fiber-like micelles in a selective solvent, the preformed micelles act as seeds which increase in length as the new polymer deposits on the growing ends.<sup>21,26</sup> For many PFS diblock copolymers, seeded growth can be carried out with exquisite control. For example, with short seeds of narrow polydispersity, rod-like micelles of very uniform length can be obtained.<sup>27</sup> Normally, all of the added polymer adds uniformly to the ends of the micelles in solution.

\* Address correspondence to gguerin@chem.utoronto.ca, ian.manners@bristol.ac.uk, mwinnik@chem.utoronto.ca.

Received for review January 9, 2013 and accepted March 22, 2013.

Published online April 15, 2013  
10.1021/nn400124x

© 2013 American Chemical Society

When one type of PFS block copolymer such as PI-PFS (PI = polyisoprene) is used to form the seed, a different type of PFS block copolymer such as PFS-PDMS (PDMS = polydimethylsiloxane) can be grown off the ends to obtain novel architectures referred to as “block comicelles”.<sup>26</sup> This process can be carried out with such control that fluorescent nanoscale barcodes up to 5  $\mu\text{m}$  in length can be prepared using polymers with appropriately chosen corona chains.<sup>28</sup>

For other polymers, this level of control cannot yet be achieved. For chiral polylactide block copolymers, fiber-like micelles could be grown with lengths up to about 300 nm, but it was difficult to obtain longer structures.<sup>17</sup> For other block copolymers, one can find conditions for generating micelles with lengths on the order of 1  $\mu\text{m}$  but not under seeded growth conditions where one can control the length.<sup>14</sup> The two conclusions that we draw from these results is that the landscape for CDSA is more complex than one might initially have thought, and that one needs a deeper understanding of how self-assembly conditions affect micelle growth.

A start in this direction is provided by recent work by the Schmalz lab. They showed that the history of sample preparation plays a key role in the self-assembly of triblock copolymers with a middle (crystallizable) polyethylene (PE) block. Different solvents required heating to different temperatures to dissolve the polymer, and two distinct types of results were obtained when these solutions were cooled to room temperature. Poor solvents for molten PE required higher temperatures to dissolve the polymers. On cooling, phase separation occurred above the melting temperature of the PE block, leading to spherical micelles. Crystallization of the PE was confined to the spherical core upon cooling. In better solvents for molten PE, the dissolution temperature decreased, and the polymer underwent CDSA when hot solutions were cooled below the melting temperature of PE, forming elongated cylinders.<sup>11</sup> Even here, however, there are still strong limitations on the length and composition of the fiber-like micelles that can be formed by seeded growth.<sup>11</sup>

As a step toward developing a deeper understanding of how self-assembly conditions affect CDSA of crystalline-coil block copolymers, we have initiated a systematic study of self-assembly protocols for a series of PFS diblock copolymers. Here we describe experiments that explore how several PFS diblock copolymers behave under “self-seeding” conditions.

Self-seeding is a process unique to polymer crystals. It was discovered in the mid-1960s by Kovacs and Keller<sup>29,30</sup> as a way of forming single crystals of polymers such as polyethylene and poly(ethylene oxide). In a self-seeding process, a bulk crystalline polymer is heated slightly above its normal melting point (as determined, for example, by differential scanning

calorimetry, DSC) to yield a transparent crystalline melt, or a crystalline polymer suspension in a solvent is heated slightly above its apparent dissolution temperature to yield a clear polymer solution. Upon cooling of the melt or solution, uniform polymer crystals form. The physical origin of the self-seeding process derives from the microscopic crystallites that survive the annealing, and these surviving nuclei initiate crystal growth as the sample cools.<sup>31</sup> Mechanistically, one explains self-seeding in terms of kinetic and thermodynamic factors that affect how polymer chains pack in a crystal. Polymer crystals consist of regions with different order of chain packing and, thus, display a broad range of melting temperatures whose values depend upon the size of the crystal as well as the details of the crystallization process. The degree of the chain order (crystallinity) depends on the rate at which the crystal was grown, the age of the crystal, and its thermal history.<sup>32</sup> Thus, when bulk crystalline polymer is heated, the least crystalline domains are the first to melt, and the most ordered crystalline domains, characterized by the highest melting point, are the last to survive with increasing temperature. A similar explanation describes self-seeding for polymer crystals suspended in a good solvent.

Lotz and Kovacs<sup>33,34</sup> found that the crystalline component of diblock copolymers with one crystalline block (e.g., poly(styrene-*b*-ethylene oxide), PS-PEO) could also be induced to form single crystals by self-seeding. These were the first results to suggest that coil-crystalline block copolymers formed planar raft-like micelles in solvents selective for the noncrystalline block. In 2009, Reiter and co-workers<sup>35</sup> showed for crystalline polymers in the bulk state that the single crystals obtained by self-seeding depended only on the annealing temperature and not the length of time that the sample was heated. They concluded that self-seeding operated under thermodynamic rather than kinetic control.<sup>36–38</sup> In recent years, self-seeding has been widely used to generate uniform polymer crystals formed by coil-crystalline block copolymers for further applications.<sup>39–42</sup>

In 2010, we published a short communication<sup>43</sup> reporting the first example of a one-dimensional analogue to the self-seeding phenomenon. These experiments examined fiber-like micelles formed by the diblock copolymer PI<sub>1000</sub>-PFS<sub>50</sub>,<sup>44</sup> where the subscripts refer to the number average degree of polymerization. These micelles fragment when their solutions are subjected to relatively mild sonication, with a rate that decreases as the micelles become shorter.<sup>45</sup> To explore the analogy to self-seeding, we heated solutions of PI<sub>1000</sub>-PFS<sub>50</sub> micelle fragments in decane to temperatures above 60 °C and then cooled the solutions back to room temperature. After this treatment, we found that longer micelles of uniform length had formed, and that the length of the micelles formed in this way

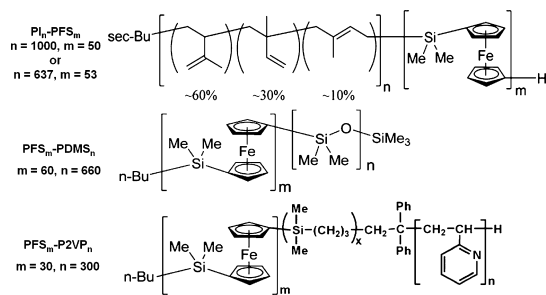
increased with the increase in heating temperature. The mass of polymer  $m$  in solution is fixed, and the amount of free polymer molecules in solution at room temperature is undetectably small.<sup>46</sup> Moreover, from our experience with this system, we know that no end-to-end attachment between the micelles occurs. Thus we conclude that the increase in the length of micelles occurred because of a decrease of the total number  $N$  of micelles in solution. This relationship is described by the expression

$$L_n = (1/m_L)(m/N) \quad (1)$$

where  $m_L$  is the mass per unit length of the micelles.

We explained this behavior from the thermodynamic perspective of self-seeding, supposing that it is the polymer less perfectly incorporated into the semi-crystalline PFS core that dissolves at a given dissolution temperature, and that higher temperatures lead to dissolution and disappearance of a greater fraction of the micelle fragment crystals. As a portion of the micelles dissolve, they form free polymer molecules in solution. These free polymer molecules grow back onto the ends of the remaining seed crystals as the solution is cooled, and the length of the micelles formed is determined by the number of remaining seed crystals as suggested by eq 1. On the basis of the initial length of the micelle fragments and final length of the micelles after heating, we calculated the fraction of the surviving seeds at various temperatures. In agreement with the findings of Reiter *et al.*<sup>35</sup> for crystalline polymer melts, we found that the fraction of the elongated micelles decreased exponentially with the increase of the dissolution temperature and did not vary with the dissolution time.

The experiments referred to in the previous paragraph<sup>43</sup> involved a single block copolymer sample under a single set of experimental conditions. In order to explore the scope of “one-dimensional” self-seeding and its generality, we have carried out new experiments, under different sets of experimental conditions, and extended these experiments to include additional samples of PFS diblock copolymers. In this paper, we describe several examples that provide more information and a deeper understanding of the self-seeding behavior of fiber-like micelles formed by crystalline-coil block copolymers. In the first example, we investigate the effect of small amounts of a good solvent for PFS (e.g., tetrahydrofuran, THF) on the self-seeding behavior of PI<sub>1000</sub>-PFS<sub>50</sub> block copolymer micelles in decane and then show that the self-seeding of PI<sub>1000</sub>-PFS<sub>50</sub> micelle fragments in decane can also be accomplished at room temperature by addition of larger amounts of THF, followed by slow selective evaporation of this solvent. In the second example, we show that the self-seeding behavior of PI<sub>1000</sub>-PFS<sub>50</sub> block copolymer micelles in decane is strongly affected by preannealing the micelle fragments. In the last set of examples, we examine the extension of the self-seeding



**Scheme 1.** Structures of PI<sub>1000</sub>-PFS<sub>50</sub>, PI<sub>637</sub>-PFS<sub>53</sub>, PFS<sub>60</sub>-PDMS<sub>660</sub>, and PFS<sub>30</sub>-P2VP<sub>300</sub>.

protocol to fiber-like micelles formed by several other PFS diblock copolymers, PI<sub>637</sub>-PFS<sub>53</sub><sup>47</sup> in decane, PFS<sub>60</sub>-PDMS<sub>660</sub><sup>47</sup> in decane, and PFS<sub>30</sub>-P2VP<sub>300</sub><sup>48</sup> in 2-propanol. The structures of these block copolymers are shown in Scheme 1. Our notation for these block copolymers reflects the sequence of synthetic steps when the block copolymers were synthesized; that is, the anionically polymerized PI block was the precursor block for PI-PFS, while for PFS-PDMS and PFS-P2VP, the PFS block was synthesized first. PI-PFS and PFS-PDMS are able to self-assemble to form long micelles in decane, a selective solvent for PI and for PDMS. In contrast, we choose 2-propanol as the selective solvent for the P2VP for the formation of long micelles by PFS-P2VP.

## RESULTS AND DISCUSSION

The sources of the polymers employed here and the experimental details of sample preparation are presented in the Methods section as well as in Supporting Information (SI). In brief, for each block polymer, a solid sample was suspended in a selective solvent and heated to a temperature (e.g., PI<sub>1000</sub>-PFS<sub>50</sub> in decane, 100 °C) at which the polymer dissolved. Upon cooling to room temperature (cooling rate *ca.* 1.5 °C/min) and aging, long micelles (>1 μm) of uniform width formed (Figure 1A). These micelle solutions were subjected to mild sonication (with an ultrasonic cleaning bath) to fragment the micelles to lengths shorter than 100 nm (Figure 1B). The micelle fragments were then subjected to the self-seeding protocol. As described in SI, we also examined samples of the block copolymers by gel permeation chromatography after subjecting them to sonication to see if sonication led to polymer degradation. For PI<sub>1000</sub>-PFS<sub>50</sub>, the extent of degradation was less than 5% (see Figure S1 in SI).

Before presenting the new experiments described below, we would like to comment on two aspects of the self-seeding phenomenon, particularly for the generation of uniform structures. These features relate to the cooling step after heating the sample to dissolve its less crystalline components. The first is that cooling the sample must generate a supersaturated solution of the polymer. Supersaturation provides the driving force for crystallization of the polymer upon cooling. The second is that self-nucleation (homonucleation) of

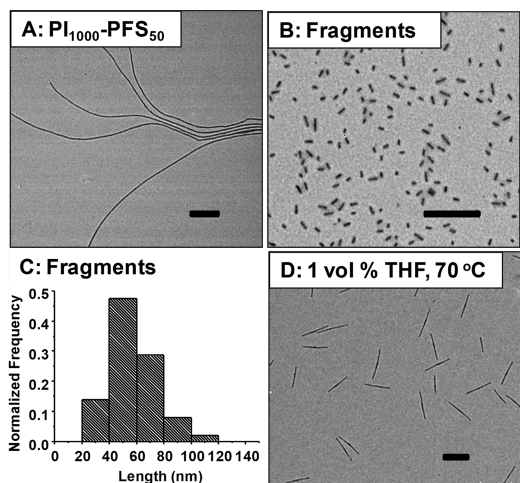


**Figure 1.** (A) PI<sub>1000</sub>-PFS<sub>50</sub> micelles formed by dissolving polymer (0.373 mg) in decane (3.73 mL,  $c = 0.100$  mg/mL) in a 20 mL vial at 100 °C for 30 min, followed by slow cooling (1.5 °C/min) to room temperature. (B) PI<sub>1000</sub>-PFS<sub>50</sub> micelle fragments obtained by sonicating the long micelles in (A) for two 10 min intervals. (C) Length distribution histogram of the micelle fragments as shown in (B).  $L_n = 57$  nm and  $L_w/L_n = 1.12$ . (D) PI<sub>1000</sub>-PFS<sub>50</sub> micelles formed by heating the fragments in decane containing 1 vol % THF to 70 °C for 30 min, followed by cooling to room temperature. Scale bars are 500 nm.

the crystals during cooling must be avoided on the time scale of the experiment. This condition can be satisfied if the experiment is carried out at sufficient dilution. If the surviving seed crystallites in the annealing step are the sole source of nuclei upon cooling, and they all grow at approximately the same rate, then uniform crystals will be formed.

**Effect of Small Amounts of Good Solvent on Self-Seeding Behavior of PI<sub>1000</sub>-PFS<sub>50</sub>.** In this section, we describe experiments that examine the effect of the presence of small amounts of THF on the self-seeding behavior of PI<sub>1000</sub>-PFS<sub>50</sub> micelle fragments in decane. THF is a good solvent for both the PFS and PI blocks. The micelle fragments were characterized by  $L_n = 57$  nm and  $L_w/L_n = 1.12$  (see the length distribution histogram in Figure 1C). Capped vials containing fragment solutions in decane containing different amounts of THF (0, 0.3, 0.6, 1.0 vol %) were heated in an oil bath at various temperatures for 30 min, allowed to cool in air, and then aged at least 1 day at room temperature. In Figure 1D, we present a representative TEM image of the PI<sub>1000</sub>-PFS<sub>50</sub> micelles obtained by heating the fragments in decane containing 1.0 vol % THF to 70 °C for 30 min, followed by cooling and aging.

In Figure 2A, we plot the number-averaged lengths ( $L_n$ ) of the micelles obtained after the heating and cooling process *versus* heating temperatures. Values of  $L_n$ ,  $L_w$ ,  $L_w/L_n$ , and  $\sigma/L_n$  of all of these samples are collected in Table S1 (SI). The data in Figure 2A show that after aliquots of each fragment solution were heated above 60 °C for 30 min and cooled to room temperature, the longer micelles obtained had lengths that were sensitively dependent on both the heating

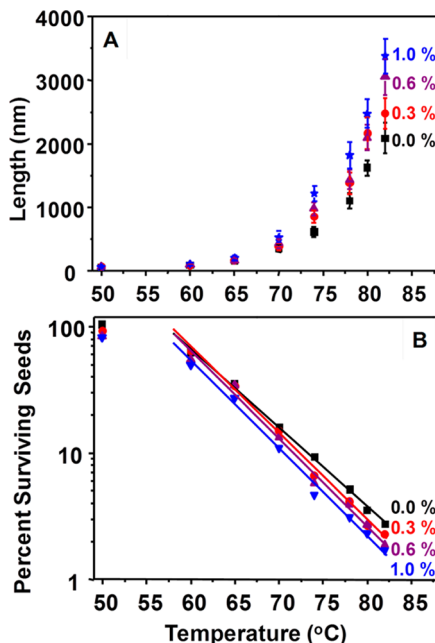


**Figure 2.** (A) Mean micelle length  $L_n$  of micelles obtained by heating the PI<sub>1000</sub>-PFS<sub>50</sub> fragment decane solutions for 30 min with the presence of different volume fractions of THF *vs* heating temperatures. (The error bars are the standard deviations  $\sigma$  for each sample calculated from the histogram of the length distributions.) (B) Semilogarithmic plots of fraction of surviving seeds in solution of PI<sub>1000</sub>-PFS<sub>50</sub> micelle fragments with different volume fractions of THF *vs* dissolution temperatures. (The solid lines represent the linear best fits for the highest several data points.).

temperatures as well as the amount of THF that was present in the solution. The length distribution of these samples remained very narrow, as shown by the standard deviation (error bars  $\sigma$ ) for each point. For the same heating temperature, the presence of THF led to the formation of longer micelles compared to the micelles obtained by heating the fragments in decane itself.

In ref 43, we described the use of eq 1 to calculate the fraction of surviving fragments at each temperature based on the final length of the micelles and the initial length of the seed fragments. The calculation took into account three features of the self-seeding process: (i) the constant mass of polymer in each solution; (ii) the negligible solubility of the polymer at room temperature; and (iii) the constant value of  $m_L$ , the mass per unit length of the micelles. For the experiments described here, the mass of polymer in each solution also remained constant, and we also assume that  $m_L$  remained constant. We also know that small amounts THF (up to 1 vol %) in decane do not lead to a measurable solubility of the polymer at room temperature.<sup>46</sup> Consequently, we can apply eq 1 to the data in Figure 2A to obtain the fraction of surviving fragments at each temperature for decane solutions containing different amounts of THF. We plot these values *versus* heating temperatures in Figure 2B. One sees that, for each solution, the fraction of surviving fragments decreased exponentially with the

increase of the annealing temperature. One can also see that, at the same heating temperature, the presence of increasing amounts of THF resulted in smaller fractions of surviving fragments compared to fragments in decane solution itself. In other words, the temperature required to dissolve equal fractions of fragments shifted to a smaller value when the volume fraction of THF increased. For example, the temperature required to dissolve 97% of the micelle fragments (3% surviving fragments) shifted from *ca.* 82 °C (fragments in pure decane) to *ca.* 78 °C (in 1 vol % THF in decane).

We discuss these results from a qualitative perspective in terms of eq 2 originally developed by Flory *et al.*<sup>49</sup> to explain the influence of solvent on the melting temperature of semicrystalline polymers.

$$\frac{1}{T_m} - \frac{1}{T_m^0} = (R/\Delta H_f) \frac{V_u}{V_1} (\varphi_1 - \chi \varphi_1^2) \quad (2)$$

Here  $T_m^0$  is the melting point of the pure polymer,  $\Delta H_f$  is the heat of fusion per polymer repeat unit,  $V_u$  is the molar volume of the polymer repeat unit,  $V_1$  is the molar volume of the solvent, and  $\varphi_1$  is the volume fraction of the solvent;  $\chi$  is the Flory–Huggins parameter that describes the quality of the solvent for the polymer: good solvents have values of  $\chi < 0.5$ .

Before discussing how this equation applies to the data in Figure 2, we would like to point out that this equation provides a framework for understanding why the dissolution (melting) temperature of the micelles in decane is lower than the melting temperature of the PFS core of the micelles in the dry state. In Figure S2, we present a series of AFM images of  $\text{PI}_{1000}\text{-PFS}_{50}$  on a mica substrate at increasing temperatures. These images show that the PFS core melts in the range of 130 to 145 °C, close to the melting temperature of bulk PFS homopolymer.<sup>50</sup> In contrast, these micelles dissolve in decane when heated in the range of 90 to 100 °C. In the context of eq 2, we imagine that, at room temperature, decane may swell the amorphous domains of the semicrystalline PFS core but does not penetrate into the crystalline phase. The magnitude of  $\chi$  decreases as the solution is heated, increasing the extent of swelling of the amorphous PFS domains. At the dissolution temperature, melting is also promoted by the entropy of mixing of the PFS block with the large excess of decane solvent.<sup>51</sup>

THF is a good solvent for PFS. When small amounts of THF are present in the decane, it likely becomes enriched in the amorphous PFS domains and contributes to the effective  $\chi$  parameter in eq 2. Again, the magnitude of  $\chi$  decreased as the temperature was increased, promoting the melting of the PFS core of the micelle. The fact that we obtain similar plots in Figure 2B for solutions containing different amounts of THF indicates that dissolution (melting) is shifted to lower temperatures for all of these fragments in the presence of increasing amounts of THF. The presence of the good solvent does not change the fundamentals

of the self-seeding process: less crystalline fragments dissolve at lower temperatures, and more crystalline fragments survive in solution to higher temperatures.

#### Solvent-Induced Self-Seeding of $\text{PI}_{1000}\text{-PFS}_{50}$ at Constant Temperature.

In the previous section, we saw that adding small amounts of THF (a good solvent) to decane reduced the dissolution temperature for the micelle seeds. We infer that, at a given temperature, the presence of THF in decane increases the degree of supersaturation of the polymer. This result raises the question of whether a good solvent might be used at room temperature to achieve a solvent-induced self-seeding protocol. To find appropriate conditions for this experiment, we need to find a supersaturation regime, a range of THF–decane mixtures where some of the micelle seeds will persist and where there will be no self-nucleation of micelles as the THF evaporates. In ref 46, we showed that adding THF to a solution of  $\text{PI}_{1000}\text{-PFS}_{50}$  micelles in decane at room temperature caused long micelles to fragment when the THF amount exceeded 11 vol %. At THF contents of 18 vol % and above, the micelles dissolved completely. To find supersaturation conditions, we took samples of the polymer dissolved in THF, added different amounts of decane, and monitored these solutions by light scattering (see Figure S3 and accompanying discussion). At low polymer concentrations ( $c = 100 \mu\text{g/mL}$ ), no spontaneous nucleation took place on a 1 week time scale for THF contents of 9 vol % or higher. Nevertheless, micelle growth could be initiated by adding short micelles as seeds. Our experiments were designed with the idea that, between 10 and 17 vol % THF, some micelle seeds will persist and that supersaturation driving crystal growth will take place as THF evaporates. We anticipated that, at 18 vol % THF, the polymer would dissolve completely.

In this section, we describe experiments in which increasing amounts of THF added to a decane solution of  $\text{PI}_{1000}\text{-PFS}_{50}$  micelle fragments led to selective dissolution of some of the fragments. Slow evaporation of the THF at room temperature (23 °C) led to regrowth of the micelles with lengths sensitively dependent on the THF content of the solvent mixture. We chose a  $c = 20 \mu\text{g/mL}$  to ensure that no spontaneous nucleation of micelles would occur during THF evaporation. We prepared nine samples of  $\text{PI}_{1000}\text{-PFS}_{50}$  micelle fragments in decane/THF mixtures containing 10 to 18 vol % THF. After 2 h at room temperature, the samples in loosely capped vials were placed in a desiccator and subjected to mild vacuum (*ca.* 10 Torr for 12 h) to evaporate the THF. A control sample containing 19 vol % THF in decane but no polymer was included to allow us to measure the loss of THF. A  $^1\text{H}$  NMR spectrum of the control sample (Figure S4) showed that, after 12 h, the THF content of the solvent had dropped to 0.4 vol %.

In Figure 3A, we plot the mean micelle length  $L_n$  of the micelles obtained after the evaporation of THF *versus* the initial THF content of the solution. These

values increased from 57 nm at low THF content, the length of the seed fragments, to more than 2200 nm at 17 vol % THF. The length distributions were narrow. Values of  $L_n$ ,  $L_w$ ,  $L_w/L_n$ , and  $\sigma/L_n$  for all of these samples are presented in Table S2 in SI. For the sample at 18 vol % THF, after the evaporation of THF, long micelles formed that resembled those of the initially prepared micelles, as shown in Figure 1A. We conclude that the micelle fragments dissolved completely in this solvent mixture.

The elongation of the micelles after the selective evaporation of THF resembles a self-seeding event. In an analogy to temperature-induced self-seeding, we infer that the addition of THF increased the solubility of the block copolymer, leading to the dissolution of micelle fragments with low crystallinity. The presence of more THF in the solution led to the dissolution of a greater fraction of the micelle fragments. As the THF evaporated, the solubility of the polymer molecules decreased, creating supersaturation conditions. Free polymer molecules in solutions grew back onto the surviving seed micelles, forming longer micelles of uniform length. In Figure 3B, we plot the fraction of surviving seeds versus the THF content of the initial solutions, calculated *via* eq 1, based on the initial length of the fragments and the final length of the micelles. One can see that, as the THF content of the solutions increased from 10 to vol 17%, the fraction of surviving seeds decreased. When the THF content was 17 vol %, the fraction of surviving seeds was only 0.02.

In previous experiments, we observed that long  $\text{PI}_{1000}\text{-PFS}_{50}$  micelles could break easily.<sup>52</sup> For example, we found that long  $\text{PI}_{1000}\text{-PFS}_{50}$  micelles with a narrow length distribution underwent rapid fragmentation when dispersed in a decane/THF mixture containing 13 vol % THF, noticeably broadening their length distribution ( $\sigma/L_n = 0.35$  after 10 min).<sup>46</sup> The results in Figure 3 show that long micelles with a remarkably narrow length distribution were obtained (Figure S5) by solvent-induced self-seeding. This result strongly suggests that much of the micelle growth in THF/decane mixtures occurred only when the amount of THF remaining in the solution was too small to promote micelle fragmentation.

These experiments show that solvent-induced self-seeding can serve as an excellent alternative to control the dissolution of semicrystalline polymer nuclei and to generate long micelles with a narrow length distribution. This approach becomes particularly useful when one cannot find an adequate range of temperatures to perform temperature-induced self-seeding.

**Effect of Preannealing on the Self-Seeding Behavior of  $\text{PI}_{1000}\text{-PFS}_{50}$ .** Annealing polymer crystals below their melting point improves their crystallinity.<sup>53,54</sup> In one of the earliest reports, Peterlin showed that annealing semicrystalline polyethylene in the bulk state led to an increase in crystal thickness and an increase of melting temperature. The rate of thickening was temperature-dependent and

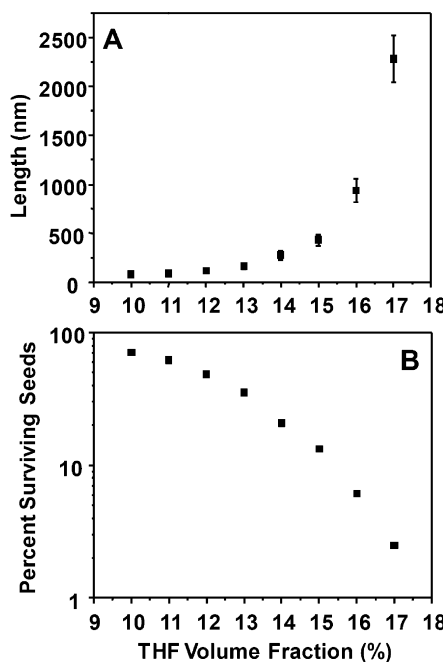


**Figure 3.** (A) Mean micelle length  $L_n$  of micelles formed after the evaporation of THF vs the volume fractions of THF in the  $\text{PI}_{1000}\text{-PFS}_{50}$  fragment solutions before the evaporation of THF. (The error bars are the standard deviations  $\sigma$  for each sample calculated from the histograms of the length distributions. The initial fragments were characterized by  $L_n = 57$  nm,  $L_w/L_n = 1.13$ .) (B) Plots of fraction of surviving seeds in solution of  $\text{PI}_{1000}\text{-PFS}_{50}$  micelle fragments vs the volume fraction of THF.

faster at higher  $T$ .<sup>55</sup> In this section, we describe self-seeding experiments on  $\text{PI}_{1000}\text{-PFS}_{50}$  micelle fragments and fragments that were preannealed at temperatures below the dissolution temperature of the micelle fragments. The preannealing of micelle fragments is expected to improve the crystallinity of the core and stability of the micelle, thus affecting the self-seeding behavior of the micelle fragments.

In these experiments, three solutions of  $\text{PI}_{1000}\text{-PFS}_{50}$  micelle fragments in decane were annealed for 24 h in an oil bath at three different temperatures (45, 50, and 55 °C), followed by cooling to room temperature. At these temperatures, there is no detectable dissolution of polymer from the micelle fragments.<sup>43</sup> We compared TEM images as well as histograms of the length and width distribution of the micelle fragments before and after annealing (cf., Figure S6). Changes in length and width were negligible.

Self-seeding experiments were then carried out on the three preannealed fragment samples in parallel with a sample of non-preannealed micelle fragments. In Figure 4A, we plot the average lengths  $L_n$  of the micelles obtained after heating the  $\text{PI}_{1000}\text{-PFS}_{50}$  fragment solutions and cooling versus heating temperatures. One sees that, after heating the solutions at temperatures above 60 °C, longer micelles with narrow length distributions were obtained. The lengths of the micelles depended sensitively on the heating temperature as well as the preannealing temperature. Preannealing led to

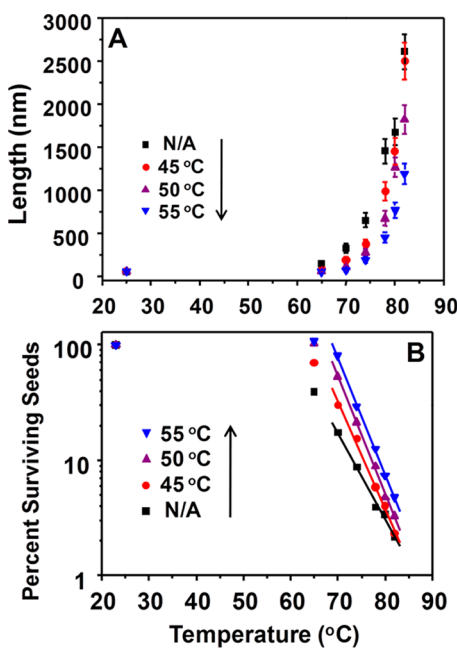


**Figure 4.** (A) Effect of preannealing on the mean length  $L_n$  of micelles obtained by heating solutions of  $\text{PI}_{1000}\text{-PFS}_{50}$  fragments in decane for 30 min at the temperatures indicated on the x-axis followed by cooling to room temperature. The initial fragments were characterized by  $L_n = 57 \text{ nm}$ ,  $L_w/L_n = 1.13$ . The symbols and corresponding colors indicate the temperature at which the fragment solution in decane was annealed for 24 h. N/A means that this set of samples was not preannealed. (B) Semilogarithmic plots of fraction of surviving seeds in solution of  $\text{PI}_{1000}\text{-PFS}_{50}$  micelle fragments vs heating temperatures. (The solid lines represent the best linear fits for the highest several data points.)

micelles of shorter length after the self-seeding experiments, and the higher the preannealing temperature, the shorter the micelles that were obtained. For example, at the highest heating temperature investigated (82 °C), micelles of  $L_n = 2600 \text{ nm}$  were obtained from the non-preannealed fragments. In contrast, the micelles obtained by the preannealed fragments (55 °C) were characterized by  $L_n = 1200 \text{ nm}$ . The values of  $L_n$ ,  $L_w$ ,  $L_w/L_n$ , and  $\sigma/L_n$  for all of these samples are collected in Table S3. These results indicate that the preannealing treatment had an important effect on the self-seeding behavior of the  $\text{PI}_{1000}\text{-PFS}_{50}$  micelle fragments.

We then used eq 1 to calculate the fraction of surviving seeds at each heating temperature for these samples (Figure 4B). One sees that, for each sample, the fraction of surviving seeds decreased exponentially with the increase of the heating temperature. At each heating temperature, the fraction of surviving seeds of the preannealed sample was larger than that of the non-preannealed sample, and preannealing at a higher temperature led to a larger fraction of surviving seeds. Comparing the data for the non-preannealed fragments and the fragments after being preannealed at 55 °C for 24 h in Figure 4B, one can see that the dissolution temperature of the micelle fragments was shifted ca. 5 °C to higher value. These results imply that

the stability (*i.e.*, the crystallinity) of the micelle fragments was improved by the preannealing treatment.

**Self-Assembly of Other PFS Block Copolymers in Selective Solvents.** In this section, we extend the self-seeding experiments to several other PFS block copolymer micelle samples and show that self-seeding is a versatile approach to generate uniform PFS fiber-like micelles. The block copolymer samples investigated in this section include  $\text{PI}_{637}\text{-PFS}_{53}$  micelles in decane,  $\text{PFS}_{60}\text{-PDMS}_{660}$  micelles in decane, and  $\text{PFS}_{30}\text{-P2VP}_{300}$  micelles in 2-propanol. 2-Propanol is good solvent for the P2VP block but a nonsolvent at room temperature for the PFS block. Micrometer-long micelle samples were obtained by heating polymer–solvent mixtures (100 °C for decane, 80 °C for  $\text{PFS}_{30}\text{-P2VP}_{300}$  in 2-propanol) as shown in Figure S7. In Figure S8, we show representative TEM images and histograms of the length distribution of the micelle fragments that resulted from sonicating these micelles. These micelles fragments were characterized by  $\text{PI}_{637}\text{-PFS}_{53}$   $L_n = 63 \text{ nm}$ ,  $L_w/L_n = 1.29$ ;  $\text{PFS}_{60}\text{-PDMS}_{660}$   $L_n = 47 \text{ nm}$ ,  $L_w/L_n = 1.12$ ;  $\text{PFS}_{30}\text{-P2VP}_{300}$   $L_n = 66 \text{ nm}$ ,  $L_w/L_n = 1.23$ .

We then annealed aliquots of the these fragment solutions in an oil bath at different temperatures for 30 min and allowed these solutions to cool back to room temperature. In Figure S9, we show representative TEM images for the three block copolymer micelle fragments annealed at different temperatures. Histograms of the length distribution are presented in Figure S10. In these experiments, we obtained longer micelles than the initial micelle fragments of each sample. These micelles had uniform widths that were identical to those of the initially prepared micelles shown in Figure S7. When the solutions were heated to higher temperatures (75 °C for  $\text{PI}_{637}\text{-PFS}_{53}$ ; 80 °C for  $\text{PFS}_{60}\text{-PDMS}_{660}$ ), long micelles formed on cooling (Figure S11), consistent with complete dissolution of the micelle fragments at these temperatures. For the  $\text{PFS}_{30}\text{-P2VP}_{300}$  sample, when heated 30 min at 80 °C, the micelles obtained upon cooling showed aggregated structures with branched morphologies, as shown in Figure S11C.

In Figure 5A,B, we plot  $L_n$  for each sample versus the annealing temperature for each micelle polymer composition. The values of  $L_n$ ,  $L_w$ ,  $L_w/L_n$ , and  $\sigma/L_n$  for all of these samples are collected in Tables S4 ( $\text{PI}_{637}\text{-PFS}_{53}$ ), S5 ( $\text{PFS}_{60}\text{-PDMS}_{660}$ ), and S6 ( $\text{PFS}_{30}\text{-P2VP}_{300}$ ). These results show that after heating the micelle fragment solutions above a certain temperature (60 °C for  $\text{PI}_{637}\text{-PFS}_{53}$ , 65 °C for  $\text{PFS}_{60}\text{-PDMS}_{660}$ , and 60 °C for  $\text{PFS}_{30}\text{-P2VP}_{300}$ ), followed by cooling to room temperature, there was a dramatic increase in the length of the micelles obtained. For the  $\text{PI}_{637}\text{-PFS}_{53}$  and  $\text{PFS}_{60}\text{-PDMS}_{660}$  samples, we obtained micelles with narrow length distributions ( $L_w/L_n < 1.04$ ). For the  $\text{PFS}_{30}\text{-P2VP}_{300}$  samples, the data point at  $T = 75$  °C in Figure 5B shows a broader length distribution ( $L_w/L_n = 1.06$ ;  $\sigma/L_n = 0.257$ ),

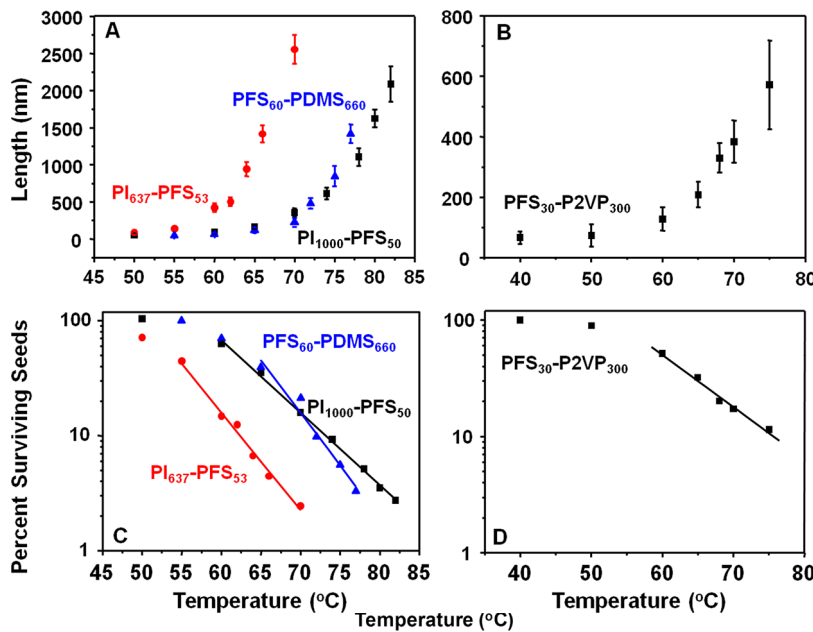


**Figure 5.** (A,B) Mean micelle length  $L_n$  vs heating temperature for (A)  $\text{PI}_{1000}\text{-PFS}_{50}$ ,  $\text{PI}_{637}\text{-PFS}_{53}$ , and  $\text{PFS}_{60}\text{-PDMS}_{660}$ , and (B)  $\text{PFS}_{30}\text{-P2VP}_{300}$ . Each fragment solution was annealed for 30 min. The error bars are the standard deviations  $\sigma$  for each sample calculated from the histograms of the length distributions. Data for  $\text{PI}_{1000}\text{-PFS}_{50}$  are taken from Figure 2A for the sample in decane containing no THF. (C,D) Semilogarithmic plots of fraction of surviving seeds in solution of (C)  $\text{PI}_{1000}\text{-PFS}_{50}$ ,  $\text{PI}_{637}\text{-PFS}_{53}$ , and  $\text{PFS}_{60}\text{-PDMS}_{660}$ , and (D)  $\text{PFS}_{30}\text{-P2VP}_{300}$  micelle fragments vs heating temperatures. (The solid lines represent the trend lines for the highest several data points.)

while the length distributions for the other data points below 75 °C are narrow ( $L_w/L_n < 1.04$ ;  $\sigma/L_n < 0.2$ ).

We attribute the elongation of the micelles to the decrease of micelle number in solution when the  $\text{PI}_{637}\text{-PFS}_{53}$ ,  $\text{PFS}_{60}\text{-PDMS}_{660}$ , and  $\text{PFS}_{30}\text{-P2VP}_{300}$  micelle fragment solutions were treated under self-seeding conditions. On the basis of the data in Figure 5A,B, we used eq 1 to calculate the fraction of surviving seeds at different heating temperatures for each sample. The results are shown in Figure 5C ( $\text{PI}_{637}\text{-PFS}_{53}$ ,  $\text{PFS}_{60}\text{-PDMS}_{660}$ ,  $\text{PI}_{1000}\text{-PFS}_{50}$ ), and 5D ( $\text{PFS}_{30}\text{-P2VP}_{300}$ ), where one sees that, as the annealing temperature was increased, the fraction of surviving seed fragments decreased exponentially. This is one of the key characteristics of self-seeding of polymer crystals as reported in ref 35. For these three block copolymers, the self-seeding protocol can also be used as a means of generating long micelles (up to 2500 nm for  $\text{PI}_{637}\text{-PFS}_{53}$  and  $\text{PI}_{1000}\text{-PFS}_{50}$ , up to 1400 nm for  $\text{PFS}_{60}\text{-PDMS}_{660}$ , and up to 500 nm for  $\text{PFS}_{30}\text{-P2VP}_{300}$ ) with narrow length distributions ( $L_w/L_n < 1.06$ ) and uniform width.

In order to investigate the effect of annealing time on the micelle length, aliquots of each  $\text{PI}_{637}\text{-PFS}_{53}$ ,  $\text{PFS}_{60}\text{-PDMS}_{660}$ , and  $\text{PFS}_{30}\text{-P2VP}_{300}$  fragment solutions were annealed at a fixed temperature for different lengths of time. TEM images were taken after the solutions were cooled to room temperature. The results are shown in Figure S12. The values of  $L_n$ ,  $L_w$ ,  $L_w/L_n$ , and  $\sigma/L_n$  of each sample are collected in Table S7 ( $\text{PI}_{637}\text{-PFS}_{53}$ ), Table S8 ( $\text{PFS}_{60}\text{-PDMS}_{660}$ ), and Table S9 ( $\text{PFS}_{30}\text{-P2VP}_{300}$ ) in SI. The lengths of the micelles obtained were independent of the annealing time and depended only on the

annealing temperature. This is another key characteristic of self-seeding of polymer crystals as described in ref 35.

From the plots shown in Figure 5A,C, we also learn important information about the effect of the corona-forming block on self-seeding behavior of PFS block copolymers. We focus on the three sets of experiments carried out in decane solution. For example, one can see that the dissolution temperatures of  $\text{PI}_{1000}\text{-PFS}_{50}$  seeds are about 10 °C higher than those of  $\text{PI}_{637}\text{-PFS}_{53}$  seeds. Since the length of the PFS block is the same in both block copolymers, we conclude that the increase in dissolution temperature is due the increase of the PI block length from  $\text{PI}_{637}$  to  $\text{PI}_{1000}$ . These plots also allow us to compare the behavior of  $\text{PFS}_{60}\text{-PDMS}_{660}$  seeds as a function of temperature with those of  $\text{PI}_{637}\text{-PFS}_{53}$ . Here, too, the PFS blocks are similar in length but differ in the nature of the corona-forming blocks (PDMS vs PI). We see that the  $\text{PFS}_{60}\text{-PDMS}_{660}$  seeds dissolve at higher temperatures than  $\text{PI}_{637}\text{-PFS}_{53}$  seeds. For example, only 5% of the  $\text{PI}_{637}\text{-PFS}_{53}$  starting seeds remain in solution at 65 °C, while ca. 40% of the  $\text{PFS}_{60}\text{-PDMS}_{660}$  seeds are still present in solution.

These results are surprising because the micelles formed by the more soluble block copolymer require higher temperatures to dissolve. For example, we expect  $\text{PI}_{1000}\text{-PFS}_{50}$  to be more soluble in decane than  $\text{PI}_{637}\text{-PFS}_{53}$  because of its longer PI block. We also expect  $\text{PFS}_{60}\text{-PDMS}_{660}$  to be more soluble in decane than  $\text{PI}_{637}\text{-PFS}_{53}$  because decane is a better solvent for PDMS than for PI, as reflected in their solubility parameters (PDMS,  $\delta = 16.6 \text{ MPa}^{1/2}$ ; PI,  $\delta = 17.0 \text{ MPa}^{1/2}$ ; decane,  $\delta = 15.8 \text{ MPa}^{1/2}$ ). However, the fragments of the micelles

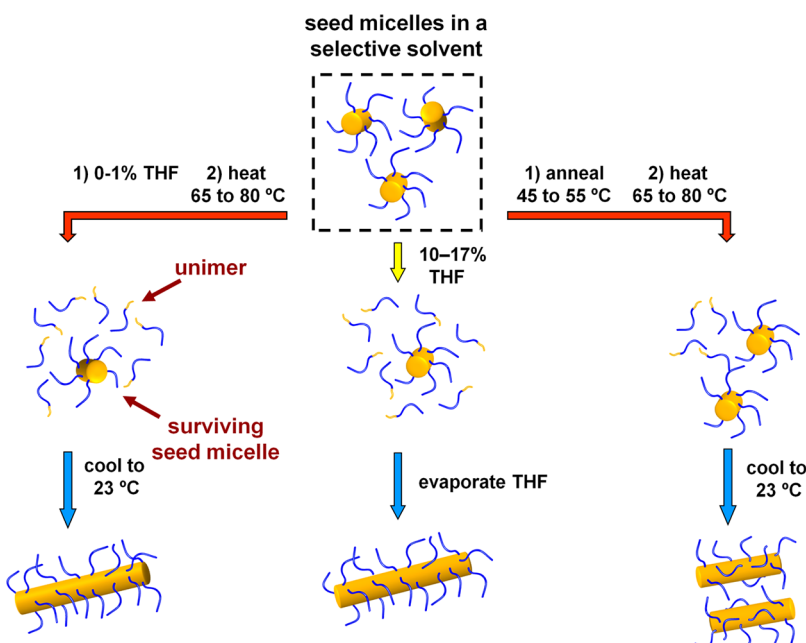


**Figure 6.** Self-seeding protocols used to prepare solutions of long micelles, narrowly distributed in length. At the left, we show how to obtain long uniform micelles by heating short seed micelles in a selective solvent for the non PFS block (with or without small amounts of THF present) and allowing the solution to cool to room temperature. In the center, we show solvent-induced self-seeding, performed by adding different amounts of THF (10 to 17%) to a decane solution of seed micelles, followed by evaporating THF under mild vacuum. On the right, we show that, by preannealing the micelles seeds in solution, we improve their crystallinity and increase the range of temperatures at which they dissolve. At a similar temperature to samples on the left side of the figure, a smaller fraction of the annealed seeds would dissolve, leading to the formation of shorter micelles than those formed by seed micelles without preannealing.

formed by the more soluble block copolymers are harder to dissolve and require higher dissolution temperatures than those formed by less soluble block copolymers.

To explain this behavior, we assume that these differences in dissolution temperature reflect differences in the crystallization of the PFS block when the micelles were originally prepared. Thus we look for explanations in terms of how the nature of the corona chain could affect the formation of the semicrystalline PFS core during micelle nucleation and growth. From a simple-minded perspective, one might imagine that the more soluble the block copolymer, the slower the rate of crystallization, allowing more time for the PFS chains to pack in the micelle core.

The theory of Sanchez and DiMarzio<sup>56–58</sup> describes chain folding during polymer crystallization from solution. They proposed that, as new polymer chains add to the growing face of a polymer crystal, parts of the polymer not incorporated into the crystal protrude into solution. They called these segments “cilia”. In their model, Sanchez and DiMarzio distinguished two different types of cilia. Primary cilia consist of dangling chains which do not incorporate into the crystal. Secondary cilia consist of dangling chains that result from the interruption of chain folding by the incorporation of a new chain in the growing crystal.

Primary cilia are most often associated with long homopolymer chains. They play no role in stabilizing the crystal but can retard the approach of new polymer molecules to the growing face of the crystal. In our PFS

block copolymers, we imagine that the soluble corona block serves a role similar to that of primary cilia. For example, previous work from our group<sup>44</sup> has shown that the length and the nature of the corona-forming block of a PFS-based block copolymer can affect the mass per unit length ( $m_L$ ) of the micelles, or in other words, that it can affect how the chains pack along the micelles' core during the micelle growth. We showed that a long corona-forming block would decrease  $m_L$ . The concept of secondary cilia may also be important here, as it would refer to the way in which PFS chains fold as they become incorporated into the micelle. This folding could be interrupted by the incorporation of a new PFS chain in the growing crystal and lead to additional defects in the crystal. In a 2005 paper,<sup>59</sup> we suggested that the presence of amorphous defects in the crystalline micelle core would lead to an increase in the mass per unit length of the micelles.

## SUMMARY AND CONCLUSIONS

We describe experiments designed to explore the self-assembly landscape for PFS diblock copolymers in selective solvents leading to the formation of cylindrical or fiber-like micelles. In these experiments, fragments of micelles, with lengths less than 100 nm, were subjected to variations of a self-seeding protocol. For semicrystalline polymers, self-seeding refers to a process of heating a solution to the point that the crystalline material appears to dissolve and then cooling the solution to room temperature. If the annealing

temperature is not too high, some tiny crystallites survive, and these nucleate the growth of uniform polymer crystals upon cooling. We emphasize that this is a thermodynamic effect, not a kinetic effect. The size of the crystals obtained is very sensitive to the annealing temperature, reflecting the solubility of polymer in crystals of different degrees of crystal perfection, but independent of the time, the solutions are annealed. For the specific sets of experimental conditions examined here, we found that long micelles (1–2  $\mu$ m) with narrow length distribution were obtained. The length of the micelles obtained increased exponentially as the annealing temperature was increased over a narrow range, implying that the number of surviving seeds decreased exponentially with temperature. Our goal in carrying out these experiments was to try to develop a deeper understanding of the fundamental principles guiding the one-dimensional self-assembly of crystalline-coil block copolymers in solution.

Many of our experiments involved  $\text{PI}_{1000}\text{-PFS}_{50}$  micelle fragments in decane. In Figure 6, we summarize the different protocols we used to form long one-dimensional micelles with a narrow length distribution. We showed, for example, that the presence of traces of THF (up to 1%) in decane shifted micelle dissolution to lower temperatures. THF is a common good solvent for both blocks. One can understand this effect in terms of selective swelling of the PFS micelle core by the THF. A second set of experiments was carried out at room temperature, in which larger amounts of THF were added to solutions of the short micelles in decane. At 18 vol % THF, all the polymer dissolved, but we found a narrow range of solvent mixtures (12–17%) in which most of the micelle fragments dissolved but generated long micelles of uniform length when the THF was allowed to evaporate. The final micelle length depended sensitively on the amount of THF in the original solvent mixture. On one hand, these experiments show that one-dimensional self-seeding can be driven by solvent composition and not just by variation of temperature. More important, they show that mixed solvent have a role in temperature-driven self-seeding. This strategy may prove valuable for polymers in which the range of temperatures that can be used is limited. For example, one can imagine examples in which heating a sample of seed crystals in a poor solvent leads to melting prior to dissolution. Mixed solvents can lower the temperature needed to dissolve a significant fraction of the seed crystals and still permit crystal growth upon cooling.

A third set of experiments examined the effect of preannealing solutions of the micelle fragments in decane at low enough temperatures (45–55 °C) that no significant

self-seeding occurs. As shown in Figure 4, these preannealed micelles exhibited self-seeding behavior, but the dissolution for the preannealed micelles was shifted to higher temperatures. This effect was more pronounced for micelle fragments preannealed at the higher temperatures. Preannealing appeared to increase the degree of crystallinity of the PFS core of these micelles, and higher temperatures were needed to dissolve these crystallites in decane.

An interesting consequence of these experiments is that they show that the concept of a critical micelle concentration (CMC) or a critical micelle temperature (CMT) for block copolymer micelles breaks down for micelles with a semicrystalline core. For traditional surfactants and for many block copolymers, the CMC refers to the unimer concentration representing (at a given temperature) the onset of aggregation as solutions become more concentrated and the dissociation of aggregates when the solutions are diluted. Analogously, for a micelle solution being heated, the CMT refers (for that concentration) to the temperature at which micelles dissociate into unimers. In the work, we have described that block copolymer micelle fragments, with a semicrystalline core, consist of a distribution of species with different degrees of crystallinity. They dissolve at different temperatures or in the presence of different amounts of a good solvent for the core polymers. The dissolution or dissociation of a micelle crystallite is a function of its degree of crystallinity and not a collective property of the sample as a whole.

Other important insights come from an examination of the influence of polymer composition on the formation of fiber-like micelles under self-seeding conditions. When we compared  $\text{PI}_{1000}\text{-PFS}_{50}$ ,  $\text{PI}_{637}\text{-PFS}_{53}$ , and  $\text{PFS}_{60}\text{-PDMS}_{660}$  in decane, we found that the micelle fragments of the polymer that one would expect to have the lowest solubility ( $\text{PI}_{637}\text{-PFS}_{53}$ ) had the lowest dissolution temperature. This leads to the suggestion that the most soluble polymers may undergo slower micelle growth at room temperature, giving the PFS chains more time to pack effectively in the semicrystalline core. This is a hypothesis that one may be able to test in future studies of micelle growth kinetics.

Looking to the future, we anticipate that the new self-seeding protocols and micelle behavior described above will help one to find appropriate experimental conditions for other polymers that form micelles with a semicrystalline core. Particularly interesting would be the preparation of long uniform fiber-like block copolymer micelles with a conjugated polymer as the core-forming block. In this way, one could obtain processable nanowires for emissive or electronic applications.

## METHODS

**Materials.** The  $\text{PI}_{1000}\text{-PFS}_{50}$  ( $M_n = 81\,600$  g/mol,  $M_w/M_n = 1.02$ ),  $\text{PI}_{637}\text{-PFS}_{53}$  ( $M_n = 56\,300$  g/mol,  $M_w/M_n = 1.01$ ),

$\text{PFS}_{60}\text{-PDMS}_{660}$  ( $M_n = 63\,700$  g/mol,  $M_w/M_n = 1.06$ ), and  $\text{PFS}_{30}\text{-P2VP}_{300}$  ( $M_n = 30\,400$  g/mol,  $M_w/M_n = 1.17$ ) block copolymers were synthesized by sequential anionic polymerization

in THF as described for other PI-PFS,<sup>60</sup> PFS-PDMS,<sup>61</sup> and PFS-P2VP<sup>62</sup> samples. The PI<sub>1000</sub>-PFS<sub>50</sub> sample is the same sample described in ref 44. The PI<sub>637</sub>-PFS<sub>53</sub> sample and the PFS<sub>60</sub>-PDMS<sub>660</sub> sample are the same samples described in ref 47. The PFS<sub>30</sub>-P2VP<sub>300</sub> sample is the same sample described in ref 48.

**Effect of Good Solvent on Self-Seeding Behavior of PI<sub>1000</sub>-PFS<sub>50</sub>.** A micelle solution of PI<sub>1000</sub>-PFS<sub>50</sub> was prepared by heating polymer (0.373 mg) in decane (3.73 mL,  $c = 100 \mu\text{g/mL}$ ) in a 20 mL vial at 100 °C for 30 min in an oil bath on top of a hot plate, followed by slow cooling to room temperature (the cooling rate was approximately 1.5 °C/min). The solution was stored in the dark. One day later, the vial containing the solution was placed in 70 W ultrasonic cleaning bath and sonicated for two 10 min intervals at 23 °C. After sonication, the PI<sub>1000</sub>-PFS<sub>50</sub> fragment solution was diluted with decane to  $c = 20 \mu\text{g/mL}$ . Four equivalent batches (3.00 mL,  $c = 20 \mu\text{g/mL}$ ) of the fragment solutions were transferred to four new 7 mL vials, followed by addition of different amounts of THF, 0, 9, 18, and 30  $\mu\text{L}$ . As a result, these solutions in decane contained 0, 0.3, 0.6, and 1.0 vol % THF. Then eight 300 mg aliquots of each solution were transferred to new 7 mL vials and sealed. Four sets of vials containing the four different solvent compositions were heated in parallel for 30 min in an oil bath, and these experiments were repeated at each of eight different temperatures. After removing the samples from the oil bath, they were allowed to cool to room temperature in air and then to age at room temperature for 24 h. Aliquots of each solution were taken for TEM analysis.

**Solvent-Induced Self-Seeding of PI<sub>1000</sub>-PFS<sub>50</sub>.** PI<sub>1000</sub>-PFS<sub>50</sub> micelle fragments (decane,  $c = 20 \mu\text{g/mL}$ ) employed in the experiments described in this section were prepared in the same way as described in the previous section. Ten equivalent batches (1.00 mL) of the fragment solution were transferred to new vials (7 mL), followed by the addition of different amounts of THF, 0, 110, 124, 136, 149, 163, 176, 190, 205, and 220  $\mu\text{L}$ . As a result, these solutions contained different amounts of THF (0, 10, 11, 12, 13, 14, 15, 16, 17, 18 vol %). Two hours after the addition of THF, the 10 vials were placed in a desiccator with a cap set on top of each vial, but not tightened. Then a mild vacuum (*ca.* 10 Torr) was applied for 12 h to evaporate the THF. Another vial in the desiccator contained a solvent mixture of decane and THF (20 vol % THF) without polymer. It was used to check whether the THF had completely evaporated under these conditions. <sup>1</sup>H NMR measurements on this sample showed <0.5 mol % remaining THF peaks. Grids for TEM measurements were prepared after the vials were removed from the desiccator.

**Effect of Preannealing on Self-Seeding Behavior of PI<sub>1000</sub>-PFS<sub>50</sub>.** A new sample of PI<sub>1000</sub>-PFS<sub>50</sub> micelle fragments in decane was prepared in the same way as described above. To investigate the effect of preannealing, three equivalent batches of micelle fragment solutions (3.00 mL,  $c = 20 \mu\text{g/mL}$ ) were transferred to new vials and annealed for 24 h in an oil bath at three different temperatures (45.0, 50.0, and 55.0 °C). Each sample was then taken out of its oil bath, allowed to cool to room temperature, and aged in air for 24 h. Next, the self-seeding protocol described above was applied to these solutions by heating aliquots (0.3 g) of each sample at different temperatures (65.0, 70.0, 74.0, 78.0, 80.0, 82.0 °C) for 30 min, followed by cooling to room temperature. Grids for TEM measurements were prepared after these solutions were allowed to age at room temperature for 24 h.

**Self-Seeding of Other PFS Block Copolymers in Selective Solvents.** A micelle solution of PI<sub>637</sub>-PFS<sub>53</sub> was prepared by heating polymer (0.552 mg) in decane (5.52 mL,  $c = 100 \mu\text{g/mL}$ ) in a 20 mL vial at 100 °C for 30 min in an oil bath on top of a hot plate. A micelle solution of PFS<sub>60</sub>-PDMS<sub>660</sub> was prepared by dissolving polymer (0.567 mg) in decane (5.67 mL,  $c = 100 \mu\text{g/mL}$ ) in a 20 mL vial at 100 °C for 30 min. A micelle solution of PFS<sub>30</sub>-P2VP<sub>300</sub> was prepared by dissolving polymer (0.260 mg) in 2-propanol (2.60 mL,  $c = 100 \mu\text{g/mL}$ ) in a 20 mL vial at 80 °C for 30 min. After heating these solutions for 30 min, the heater was turned off and the solutions were allowed to cool slowly to room temperature (the cooling rate was approximately 1.5 °C/min). One day later, each solution in turn was placed in a 70 W ultrasonic cleaning bath and sonicated for 10 min at 23 °C followed by an additional 10 min at 23 °C. All of the fragment solutions were diluted with decane or 2-propanol to  $c = 20 \mu\text{g/mL}$ .

To investigate the self-seeding behavior of these block copolymers, equivalent batches containing *ca.* 300 mg fragment solutions of each sample were transferred to new vials (7 mL). These solutions were then annealed in an oil bath at various temperatures. After 30 min, each sample was taken out of the oil bath and allowed to cool to room temperature in air. These solutions were then allowed to age at room temperature for 24 h before grids for TEM measurements were prepared.

To investigate the effect of annealing time, three 300 mg PI<sub>637</sub>-PFS<sub>53</sub> fragment solutions were annealed in an oil bath at 64.0 °C for different lengths of time (10 min, 2 h, and 24 h). Similar experiments were carried out for the PFS<sub>60</sub>-PDMS<sub>660</sub> fragment solutions annealing at 75.0 °C and the PFS<sub>30</sub>-P2VP<sub>300</sub> fragment solutions annealing at 68.0 °C for different times.

**Sonication, Heating Bath, and Temperature Control.** Micelles were sonicated by immersing a vial into water at 23 °C in a BRANSON model 1510 70 W ultrasonic cleaning bath. All heating experiments were performed by placing the sample containing vials in a silicon oil bath on top of a hot plate. The temperature of the oil bath was controlled by an IKATRON ETS-D5 (Germany) thermometer with a rated temperature fluctuation of control  $\pm 0.1$  °C.

**Transmission Electron Microscopy Measurements and Data Analysis.** Transmission electron microscopy (TEM) images were taken using a Hitachi H-7000 TEM instrument. Micelle length distributions were determined using the software program ImageJ from the National Institutes of Health. For each sample, more than 200 micelles in several images were traced by the software in order to obtain the length information. The number average micelle length ( $L_n$ ) and weight average micelle length ( $L_w$ ) were calculated using eq 3 from measurements of the contour lengths ( $L_i$ ) of individual micelles, where  $N_i$  is the number of micelles of length  $L_i$ , and  $n$  is the number of micelles examined in each sample.

$$L_n = \frac{\sum_{i=1}^n N_i L_i}{\sum_{i=1}^n N_i} \quad (3)$$

$$L_w = \frac{\sum_{i=1}^n N_i L_i^2}{\sum_{i=1}^n N_i L_i}$$

The distribution of micelle lengths is characterized by both  $L_w/L_n$  and the ratio  $\sigma/L_n$ , where  $\sigma$  is the standard deviation of the length distribution.

**Conflict of Interest:** The authors declare no competing financial interest.

**Acknowledgment.** The authors thank the Natural Sciences Engineering Research Council of Canada for their support of this research. I.M. thanks the EU for a European Research Council (ERC) Advanced Investigator Grant.

**Supporting Information Available:** Additional experimental details; GPC traces of the PI<sub>1000</sub>-PFS<sub>50</sub> polymer before and after sonication (Figure S1); AFM images of PI<sub>1000</sub>-PFS<sub>50</sub> on mica as they are heated (Figure S2); evolution of the scattering intensity at 90° of PI<sub>1000</sub>-PFS<sub>50</sub> block copolymer dispersed in different vol % THF fraction in decane–THF mixtures (Figure S3); <sup>1</sup>H NMR spectra of a decane–THF mixture before and after the evaporation of THF (Figure S4); length distribution histograms of micelles obtained by solvent-induced self-seeding (Figure S5); TEM images of PI<sub>1000</sub>-PFS<sub>50</sub> micelle fragments before and after preannealing at different temperatures, with corresponding length and width distribution histograms (Figure S6); TEM images of PI<sub>637</sub>-PFS<sub>53</sub> and PFS<sub>60</sub>-PDMS<sub>660</sub> micelles in decane, PFS<sub>30</sub>-P2VP<sub>300</sub> micelles in 2-propanol, and corresponding width distribution histograms (Figure S7); TEM images of their micelle fragments (Figure S8); as well as of the micelles formed by the self-seeding protocol (Figure S9) and their length distribution histograms (Figure S10); TEM images of the micelles formed by heating each of these micelle fragment solution at higher temperatures and cooling to room temperature (Figure S11); plots showing the time dependence of micelle length formed

from solutions of  $\text{PI}_{637}\text{-PFS}_{53}$ ,  $\text{PFS}_{60}\text{-PDMS}_{660}$ , and  $\text{PFS}_{30}\text{-P2VP}_{300}$  micelle fragments after being annealed at a fixed temperatures and then cooled to room temperature in air (Figure S12); and tables (Tables S1–S9) that collect length information for all of the samples described in this paper. This material is available free of charge via the Internet at <http://pubs.acs.org>.

## REFERENCES AND NOTES

- He, W.-N.; Xu, J.-T. Crystallization Assisted Self-Assembly of Semicrystalline Block Copolymers. *Prog. Polym. Sci.* **2012**, *37*, 1350–1400.
- Bellas, V.; Rehahn, M. Polyferrocenylsilane-Based Polymer Systems. *Angew. Chem.* **2007**, *119*, 5174–5197; *Angew. Chem., Int. Ed.* **2007**, *46*, 5082–5104.
- Whittell, G. R.; Hager, M. D.; Schubert, U. S.; Manners, I. Functional Soft Materials from Metallocopolymers and Metallosupramolecular Polymers. *Nat. Mater.* **2011**, *10*, 176–188.
- Korczagin, I.; Lammertink, R. G. H.; Hempenius, M. A.; Golze, S.; Vancso, G. J. Surface Nano- and Microstructuring with Organometallic Polymers. *Adv. Polym. Sci.* **2006**, *200*, 91–117.
- Massey, J. A.; Temple, K.; Cao, L.; Rharbi, Y.; Raez, J.; Winnik, M. A.; Manners, I. Self-Assembly of Organometallic Block Copolymers: The Role of Crystallinity in the Core-Forming Polyferrocene Block in the Micellar Morphologies Formed by Poly(ferrocenylsilane-*b*-dimethylsiloxane) in *n*-Alkane Solvents. *J. Am. Chem. Soc.* **2000**, *122*, 11577–11584.
- Cao, L.; Manners, I.; Winnik, M. A. Influence of the Interplay of Crystallization and Chain Stretching on Micellar Morphologies: Solution Self-Assembly of Coil-Crystalline Poly(isoprene-block-ferrocenylsilane). *Macromolecules* **2002**, *35*, 8258–8260.
- Gilroy, J. B.; Rupar, P. A.; Whittell, G. R.; Chabanne, L.; Terrill, N. J.; Winnik, M. A.; Manners, I.; Richardson, R. M. Probing the Structure of the Crystalline Core of Field-Aligned, Monodisperse, Cylindrical Polyisoprene-*b*-Polyferrocenylsilane Micelles in Solution Using Synchrotron Small- and Wide-Angle X-ray Scattering. *J. Am. Chem. Soc.* **2011**, *133*, 17056–17062.
- Qian, J. S.; Zhang, M.; Manners, I.; Winnik, M. A. Nanofiber Micelles from the Self-Assembly of Block Copolymers. *Trends Biotechnol.* **2010**, *28*, 84–92.
- Yin, L.; Lodge, T. P.; Hillmyer, M. A. A Stepwise “Micellization–Crystallization” Route to Oblate Ellipsoidal, Cylindrical, and Bilayer Micelles with Polyethylene Cores in Water. *Macromolecules* **2012**, *45*, 9460–9467.
- Schmalz, H.; Schmelz, J.; Drechsler, M.; Yuan, J.; Walther, A.; Schweimer, K.; Mihut, A. M. Thermo-Reversible Formation of Wormlike Micelles with a Microphase-Separated Corona from a Semicrystalline Triblock Terpolymer. *Macromolecules* **2008**, *41*, 3235–3242.
- Schmelz, J.; Karg, M.; Hellweg, T.; Schmalz, H. General Pathway toward Crystalline-Core Micelles with Tunable Morphology and Corona Segregation. *ACS Nano* **2011**, *5*, 9523–9534.
- Schmelz, J.; Schedl, A. E.; Steinlein, C.; Manners, I.; Schmalz, H. Length Control and Block-Type Architectures in Wormlike Micelles with Polyethylene Cores. *J. Am. Chem. Soc.* **2012**, *134*, 14217–14225.
- Mihut, A. M.; Drechsler, M.; Möller, M.; Ballauff, M. Sphere-to-Rod Transition of Micelles Formed by the Semicrystalline Polybutadiene-*b*-Poly(ethylene oxide) Block Copolymer in a Selective Solvent. *Macromol. Rapid Commun.* **2010**, *31*, 449–453.
- Du, Z. X.; Xu, J. T.; Fan, Z. Q. Micellar Morphologies of Poly( $\epsilon$ -caprolactone)-*b*-Poly(ethylene oxide) Block Copolymers in Water with a Crystalline Core. *Macromolecules* **2007**, *40*, 7633–7637.
- He, W. N.; Zhou, B.; Xu, J. T.; Du, B. Y.; Fan, Z. Q. Two Growth Modes of Semicrystalline Cylindrical Poly( $\epsilon$ -caprolactone)-*b*-Poly(ethylene oxide) Micelles. *Macromolecules* **2012**, *45*, 9768–9778.
- Zhang, J.; Wang, L. Q.; Wang, H. J.; Tu, K. H. Micellization Phenomena of Amphiphilic Block Copolymers Based on Methoxy Poly(ethylene glycol) and Either Crystalline or Amorphous Poly(caprolactone-*b*-lactide). *Biomacromolecules* **2006**, *7*, 2492–2500.
- Petzetakis, N.; Dove, A. P.; O'Reilly, R. K. Cylindrical Micelles from the Living Crystallization-Driven Self-Assembly of Poly(lactide)-Containing Block Copolymers. *Chem. Sci.* **2011**, *2*, 955–960.
- Petzetakis, N.; Walker, D.; Dove, A. P.; O'Reilly, R. K. Crystallization-Driven Sphere-to-Rod Transition of Poly(lactide)-*b*-Poly(acrylic acid) Diblock Copolymers: Mechanism and Kinetics. *Soft Matter* **2012**, *8*, 7408–7414.
- Lazzari, M.; Scalarone, D.; Vazquez-Vazquez, C.; López-Quintela, M. A. Cylindrical Micelles from the Self-Assembly of Polyacrylonitrile-Based Diblock Copolymers in Nonpolar Selective Solvents. *Macromol. Rapid Commun.* **2008**, *29*, 352–357.
- Gädt, T.; Schacher, F. H.; McGrath, N.; Winnik, M. A.; Manners, I. Probing the Scope of Crystallization-Driven Living Self-Assembly: Studies of Diblock Copolymer Micelles with a Polyisoprene Corona and a Crystalline Poly(ferrocenylidethylsilane) Core-Forming Metallocblock. *Macromolecules* **2011**, *44*, 3777–3786.
- Gädt, T.; leong, N. S.; Cambridge, G.; Winnik, M. A.; Manners, I. Complex and Hierarchical Micelle Architectures from Diblock Copolymers Using Living, Crystallization-Driven Polymerizations. *Nat. Mater.* **2009**, *8*, 144–150.
- Patra, S. K.; Ahmed, R.; Whittell, G. R.; Lunn, D. J.; Dunphy, E. L.; Winnik, M. A.; Manners, I. Cylindrical Micelles of Controlled Length with a  $\pi$ -Conjugated Polythiophene Core via Crystallization-Driven Self-Assembly. *J. Am. Chem. Soc.* **2011**, *133*, 8842–8845.
- Lee, E.; Hammer, B.; Kim, J. K.; Page, Z.; Emrick, T.; Hayward, R. C. Hierarchical Helical Assembly of Conjugated Poly(3-hexylthiophene)-*b*-Poly(3-triethylene glycol thiophene) Diblock Copolymers. *J. Am. Chem. Soc.* **2011**, *133*, 10390–10393.
- Gao, Y.; Li, X. Y.; Hong, L. Z.; Liu, G. J. Mesogen-Driven Formation of Triblock Copolymer Cylindrical Micelles. *Macromolecules* **2012**, *45*, 1321–1330.
- We use the term “fiber-like micelle” to convey the sense of an elongated structure with a narrow width. Taking into account the long solvent-swollen corona chains that fill space around the micelle core, the overall shape is cylindrical. A more subtle question is the shape of the core. The theoretical model of Vilgis and Halperin for micelles formed by coil-crystalline block copolymers assumes that the semicrystalline cores of such micelles are lamellae, which may in fact be square, rectangular, or hexagonal in cross section. This is remarkably difficult to establish experimentally. Vilgis, T.; Halperin, A. Aggregation of Coil-Crystalline Block Copolymers: Equilibrium Crystallization. *Macromolecules* **1991**, *24*, 2090–2095. We have cryo-sectioned one sample of fiber-like PFS-PI block copolymer micelles and found the core cross section to appear round. Resolution was limited, and there may have been artifacts associated with the sectioning. Wang, X.; Liu, K.; Arseneault, A. C.; Rider, D. A.; Ozin, G. A.; Winnik, M. A.; Manners, I. Shell-Cross-Linked Cylindrical Polyisoprene-*b*-Polyferrocenylsilane (PI-*b*-PFS) Block Copolymer Micelles: One-Dimensional (1D) Organometallic Nanocylinders. *J. Am. Chem. Soc.* **2007**, *129*, 5630–5639. For all of the examples cited here and reported in this paper, the cross sectional shape of the micelle core remains unknown.
- Wang, X. S.; Guerin, G.; Wang, H.; Wang, Y. S.; Manners, I.; Winnik, M. A. Cylindrical Block Copolymer Micelles and Co-micelles of Controlled Length and Architecture. *Science* **2007**, *317*, 644–647.
- Gilroy, J. B.; Gädt, T.; Whittell, G. R.; Chabanne, L.; Mitchels, J. M.; Richardson, R. M.; Winnik, M. A.; Manners, I. Monodisperse Cylindrical Micelles by Crystallization-Driven Living Self-Assembly. *Nat. Chem.* **2010**, *2*, 566–570.
- He, F.; Gädt, T.; Manners, I.; Winnik, M. A. Fluorescent “Barcode” Multiblock Co-micelles via the Living Self-Assembly of Di- and Triblock Copolymers with a Crystalline Core-Forming Metallocblock. *J. Am. Chem. Soc.* **2011**, *133*, 9095–9103.
- Blundell, D. J.; Keller, A.; Kovacs, A. J. A New Self-Nucleation Phenomenon and Its Application to the Growing of

Polymer Crystals from Solution. *J. Polym. Sci., Part B: Polym. Lett.* **1966**, *4*, 481–486.

30. Blundell, D. J.; Keller, A. Nature of Self-Seeding Polyethylene Crystal Nuclei. *J. Macromol. Sci., Part B: Phys.* **1968**, *2*, 301–336.

31. Bassett, D. C. *Principles of Polymer Morphology*; Cambridge University Press: Oxford, UK, 1981.

32. Strobl, G. Crystallization and Melting of Bulk Polymers: New Observations, Conclusions and a Thermodynamic Scheme. *Prog. Polym. Sci.* **2006**, *31*, 398–442.

33. Lotz, B.; Kovacs, A. J. Properties of Copolymers Composed of Poly(ethylene oxide)polystyrene Sequences. I. Preparation, Composition, and Microscopic Investigation of Single Crystals. *Kolloid-Z. Z. Polym., Suppl.* **1966**, *209*, 97–114.

34. Lotz, B.; Kovacs, A. J.; Bassett, G. A.; Keller, A. Properties of Copolymers Composed of One Poly(ethylene oxide) and One Polystyrene Block. II. Morphology of Single Crystals. *Kolloid-Z. Z. Polym., Suppl.* **1966**, *209*, 115–128.

35. Xu, J. J.; Yu, M.; Hu, W. B.; Rehahn, M.; Reiter, G. Cloning Polymer Single Crystals through Self-Seeding. *Nat. Mater.* **2009**, *8*, 348–353.

36. Lorenzo, A. T.; Arnal, M. L.; Sánchez, J. J.; Müller, A. J. Effect of Annealing Time on the Self-Nucleation Behavior of Semicrystalline Polymers. *J. Polym. Sci., Part B: Polym. Phys.* **2006**, *44*, 1738–1750.

37. Massa, M. V.; Lee, M. S. M.; Dalnoki-Veress, K. Crystal Nucleation of Polymers Confined to Droplets: Memory Effects. *J. Polym. Sci., Part B: Polym. Phys.* **2005**, *43*, 3438–3443.

38. Maus, A.; Hempel, E.; Thurn-Albrecht, T.; Saalwächter, K. Memory Effect in Isothermal Crystallization of Syndiotactic Polypropylene—Role of Melt Structure and Dynamics? *Eur. Phys. J. E* **2007**, *23*, 91–101.

39. Hsiao, M. S.; Chen, W. Y.; Zheng, J. X.; Van Horn, R. M.; Quirk, R. P.; Ivanov, D. A.; Thomas, E. L.; Lotz, B.; Cheng, S. Z. D. Poly(ethylene oxide) Crystallization within a One-Dimensional Defect-Free Confinement on the Nanoscale. *Macromolecules* **2008**, *41*, 4794–4801.

40. Hsiao, M. S.; Zheng, J. X.; Horn, R. M. V.; Quirk, R. P.; Thomas, E. L.; Chen, H. L.; Lotz, B.; Cheng, S. Z. D. Poly(ethylene oxide) Crystal Orientation Change under 1D Nanoscale Confinement Using Polystyrene-block-Poly(ethylene oxide) Copolymers: Confined Dimension and Reduced Tethering Density Effects. *Macromolecules* **2009**, *42*, 8343–8352.

41. Li, B.; Li, C. Y. Immobilizing Au Nanoparticles with Polymer Single Crystals, Patterning and Asymmetric Functionalization. *J. Am. Chem. Soc.* **2007**, *129*, 12–13.

42. Li, B.; Ni, C. Y.; Li, C. Y. Poly(ethylene oxide) Single Crystals as Templates for Au Nanoparticle Patterning and Asymmetrical Functionalization. *Macromolecules* **2008**, *41*, 149–155.

43. Qian, J. S.; Guerin, G.; Lu, Y. J.; Cambridge, G.; Manners, I.; Winnik, M. A. Self-Seeding in One Dimension: An Approach To Control the Length of Fiberlike Polyisoprene–Polyferrocenylsilane Block Copolymer Micelles. *Angew. Chem., Int. Ed.* **2011**, *50*, 1622–1625.

44. Cambridge, G.; Guerin, G.; Manners, I.; Winnik, M. A. Fiberlike Micelles Formed by Living Epitaxial Growth from Blends of Polyferrocenylsilane Block Copolymers. *Macromol. Rapid Commun.* **2010**, *31*, 934–938.

45. Guerin, G.; Wang, H.; Manners, I.; Winnik, M. A. Fragmentation of Fiberlike Structures: Sonication Studies of Cylindrical Block Copolymer Micelles and Behavioral Comparisons to Biological Fibrils. *J. Am. Chem. Soc.* **2008**, *130*, 14763–14771.

46. Qian, J. S.; Guerin, G.; Cambridge, G.; Manners, I.; Winnik, M. A. Seeded Growth and Solvent-Induced Fragmentation of Fiberlike Polyferrocenylsilane–Polyisoprene Block Copolymer Micelles. *Macromol. Rapid Commun.* **2010**, *31*, 928–933.

47. Rupar, P. A.; Cambridge, G.; Winnik, M. A.; Manners, I. Reversible Cross-Linking of Polyisoprene Coronas in Micelles, Block Comicelles, and Hierarchical Micelle Architectures Using Pt(0)–Olefin Coordination. *J. Am. Chem. Soc.* **2011**, *133*, 16947–19957.

48. He, F.; Gädt, T.; Jones, M.; Scholes, G. D.; Manners, I.; Winnik, M. A. Synthesis and Self-Assembly of Fluorescent Micelles from Poly(ferrocenyl-dimethylsilane-*b*-2-vinylpyridine-*b*-2,5-di(2'-ethylhexyloxy)-1,4-phenylvinylene) Triblock Copolymer. *Macromolecules* **2009**, *42*, 7953–7960.

49. Mandelkern, L.; Garrett, R. R.; Flory, P. J. Heats of Fusion of Aliphatic Polyesters. *J. Am. Chem. Soc.* **1952**, *74*, 3949–3951.

50. Lammertink, R. G. H.; Hempenius, M. A.; Manners, I.; Vancso, G. J. Crystallization and Melting Behavior of Poly(ferrocenyl-dimethylsilanes) Obtained by Anionic Polymerization. *Macromolecules* **1998**, *31*, 795–800.

51. Teraoka, I. *Polymer Solutions: An Introduction to Physical Properties*; John Wiley & Sons, Inc.: New York, 2002.

52. Qian, J.; Lu, Y.; Cambridge, G.; Guerin, G.; Manners, I.; Winnik, M. A. Polyferrocenylsilane Crystals in Nanoconfinement: Fragmentation, Dissolution, and Regrowth of Cylindrical Block Copolymer Micelles with a Crystalline Core. *Macromolecules* **2012**, *45*, 8363–8372.

53. Sperling, L. H. *Introduction to Physical Polymer Science*; John Wiley & Sons, Inc.: New York, 2006.

54. Wunderlich, B. *Macromolecular Physics: Crystal Nucleation, Growth, Annealing*; Academic: New York, 1976; Vol. 2, Chapter V.

55. Peterlin, A. Thickening of Polymer Single Crystals during Annealing. *J. Polym. Sci., Part B: Polym. Lett.* **1963**, *1*, 279–284.

56. Sanchez, I. C.; DiMarzio, E. A. Dilute Solution Theory of Polymer Crystal Growth: A Kinetic Theory of Chain Folding. *J. Chem. Phys.* **1971**, *55*, 893–908.

57. Sanchez, I. C.; DiMarzio, E. A. Dilute-Solution Theory of Polymer Crystal Growth. Some Thermodynamic and Predictive Aspects for Polyethylene. *Macromolecules* **1971**, *4*, 677–687.

58. Keller, A.; Pedemonte, E. A Study of Growth Rates of Polyethylene Single Crystals. *J. Cryst. Growth* **1973**, *18*, 111–123.

59. Guerin, G.; Raez, J.; Manners, I.; Winnik, M. A. Light Scattering Study of Rigid, Rodlike Organometallic Block Copolymer Micelles in Dilute Solution. *Macromolecules* **2005**, *38*, 7819–7827.

60. Cao, L.; Manners, I.; Winnik, M. A. Influence of the Interplay of Crystallization and Chain Stretching on Micellar Morphologies: Solution Self-Assembly of Coil-Crystalline Poly(isoprene-block-ferrocenylsilane). *Macromolecules* **2002**, *35*, 8258–8260.

61. Massey, J.; Power, K. N.; Manners, I.; Winnik, M. A. Self-Assembly of a Novel Organometallic–Inorganic Block Copolymer in Solution and the Solid State: Non-intrusive Observation of Novel Wormlike Poly(ferrocenyl-dimethylsilane)-*b*-Poly(dimethylsiloxane) Micelles. *J. Am. Chem. Soc.* **1998**, *120*, 9533–9540.

62. Wang, H.; Winnik, M. A.; Manners, I. Synthesis and Self-Assembly of Poly(ferrocenyl-dimethylsilane-*b*-2-vinylpyridine) Diblock Copolymers. *Macromolecules* **2007**, *40*, 3784–3789.